Landscape Architecture

ARTICLE

Tree-Canopy Cooling Attainment in European Functional Urban Areas

Chi Wang* **and Xi Lei**

School of Management Science and Engineering, Shandong Technology and Business University, Yantai, Shandong, 264005, China

* Correspondence: 1987323@163.com

Abstract

Adaptation to urban heat requires scientific knowledge about the magnitude of the impact of existing vegetation-induced cooling on a certain thermal threshold and the resilience of such benefits in face of uncertainty. This article introduces a tree canopy cooling attainment calculation across 601 European FUAs in the EU-27 region. The methodological computation is based on July-August 2018 Landsat 8 OLI/TIRS land surface temperature, Copernicus tree cover density, PML V2 canopy transpiration-interception evaporation rates, Global Human Settlements population density in 2015, and model evaluation against 463 NOAA weather stations as in Marando et al.[16]. The computation translates FUA cooling into target attainment, reserves, tree cover shortage equivalent and population concordance. The average cooling attained in Europe is 1.07 °C, while the range of cooling per FUA is approximately −0.4 to 2.9 °C. Out of the total number of FUAs, 281 are still below 1 °C, 208 reach 1 °C cooling, and 112 reach 1.5 °C and above, the reliable one-degree mark following the application of a 0.5 °C allowance. The cooling target attainment thresholds using canopy as reference measure are: 16%, 32% and 48% tree canopy cover respectively for 1, 2 and 3 °C cooling. Results from the model comparison showed that country-conditioned structural forms offer a better forecasting capability compared to universal models and the complete mixed effects form has the smallest RMSE and a relative improvement of 32.1% from the null model. On the population dimension, in 63% of the cases, more than half of the population live in positive-cooling FUAs while in 37% the opposite holds. These results suggest that European greening policy should differentiate between positive cooling, one-degree attainment, reliable reserves and population alignment.

Keywords: urban heat island; tree cover; urban green infrastructure; Functional Urban Areas; cooling attainment; population exposure; climate adaptation

1. Introduction

UHI phenomena occur through surface-energy exchange, heat storage, evaporative cooling, and mixing. Heat accumulates in the urban canopy layer from dense urban structures, energy-absorbing materials, urban canyon geometry, delayed radiative emissions, and artificial heating. Consequently, air temperature and surfaces in urban areas experience warming relative to surrounding environments. The scientific explanation for the urban heat phenomenon has its roots in Oke's work, which demonstrates how urban form and material affect the partition of sensible, latent, and storied heat, and the interaction of energy and radiation [21–23]. Recent remote sensing

Received: 20 July 2021; Revised: 18 October 2021; Accepted: 27 December 2021; Published: 30 March 2022.

doi: 10.70517/la20221121-02

analysis proved the potential for identifying thermal heterogeneity among different land use and land cover classes, including roofs, roads, parks, agricultural margins, river courses, and peri-urban forests [5, 33]. The issue of land surface temperature being different from pedestrian-scale air temperature is the practical challenge to measuring urban heat. Additionally, conventional weather stations do not provide sufficient spatial density to describe heat within urban areas and in their surroundings.

Excessive heat becomes problematic for European cities due to climate warming, heat wave intensification, increase in sealing fraction of urban land cover, and population exposure. Episodes of extreme temperatures correlate with increased mortality, discomfort, heat illnesses, and strong cooling demands on power plants [7, 8, 12]. Urban development exacerbates such heat risk through replacing evaporative surfaces with dense urban structures, and urban land sealing increases rapidly in Europe [10]. However, what is essential in heat adaptation is not just regional climate warming, but rather the arrangement of heat-retaining surfaces and cooling sources in the daily environment of city dwellers. Studies conducted in Lucknow and Nanchang show that land use changes and urban expansion raise urban temperatures by over one degree in parallel with urbanization [36, 44]. In other words, there is an intrinsic rationale for approaching urban heat adaptation as a spatial planning task.

Green infrastructure is a nature-based solution for the mitigation of urban heat islands in most cities. Urban trees, shrubs, grassland, urban forest, and green corridors exert various thermal effects through shading, evapotranspiration, rain interception, surface soil moisture exchange, and substitution of high heat capacity surfaces [4, 6, 31]. The most powerful cooling depends upon canopy structure and water availability. Trees can minimize radiant load and surface heating, while large parks and peri-urban forests create extended cool patches due to their cooling effect [29, 35]. There are examples of local-level empirical studies assessing tree air cooling and urban park benefits on heat islands [11, 41, 42]. Those findings inform about greening strategies but they also suggest that not every green surface can be considered as a heat reduction tool. Vegetation type, canopy cover, soil volume, plant physiology, and moisture status play a role in the functioning of green areas as thermal infrastructure.

There is a growing body of research discussing the ways to estimate urban heat mitigation by vegetation at higher levels. Various review papers emphasize the necessity to create comparable indicators of land cover, surface temperature, evapotranspiration, and human benefit for green infrastructure evaluation [2]. While some researchers focus on structural parameters like canopy cover or normalized vegetation indices, others concentrate on functional variables like evapotranspiration rate and canopy evaporation [27, 39]. Both aspects matter because vegetation coverage is meaningless without water availability; thus, there is no point in saying that a city rich in dry grass will experience cooling even during summer months. Moreover, a city with extensive dry tree canopy will face hot summers despite high canopy cover if those trees do not perform any water exchange in the air. The link between surface temperature and air temperature depends upon local morphological and meteorological peculiarities, necessitating a modeling approach based on surface temperature combined with near-ground air temperature estimation [25, 33].

The question to answer in the planning context is different from simply measuring the amount of cooling. Even if there is a positive vegetation benefit, there is no reason to believe that cooling has met an adaptation target. In addition, there are cases when one degree of cooling is achieved but the target cannot be reached again if model uncertainty is considered or a dry summer happens. Mean cooling value may mask the population discrepancy since cooling is provided to peri-urban forests, leaving the densely populated areas uncovered. Thus, it is necessary to check whether FUAs have met an adaptation target and what level of tree cover is needed to meet that target reliably. This paper proposes an indicator of target cooling and shortage of cooling within FUAs that can be used for estimating urban heat resilience.

Target cooling and shortfall within FUAs are defined as a target-reserve relationship. The aim is not only to measure the cooling effect provided by vegetation. The next step is to determine whether that effect exceeds the adaptation target, whether it is maintained at least 0.5 °C above the target, and how much tree canopy cover should be added to ensure the reliable cooling. The accuracy of the model is also checked to prevent the assumption that it would yield similar results in each country. The results are obtained in the form of urban region classes distinguished by the presence of cooling reserve.

The spatial setting of the analysis starts with Figures 1, where urban core, commuting zone surface, peri-urban vegetation, and thermal contrast serve as visual evidence that the same Functional Urban Area has varying land cover types, vegetation density, and surface temperature.

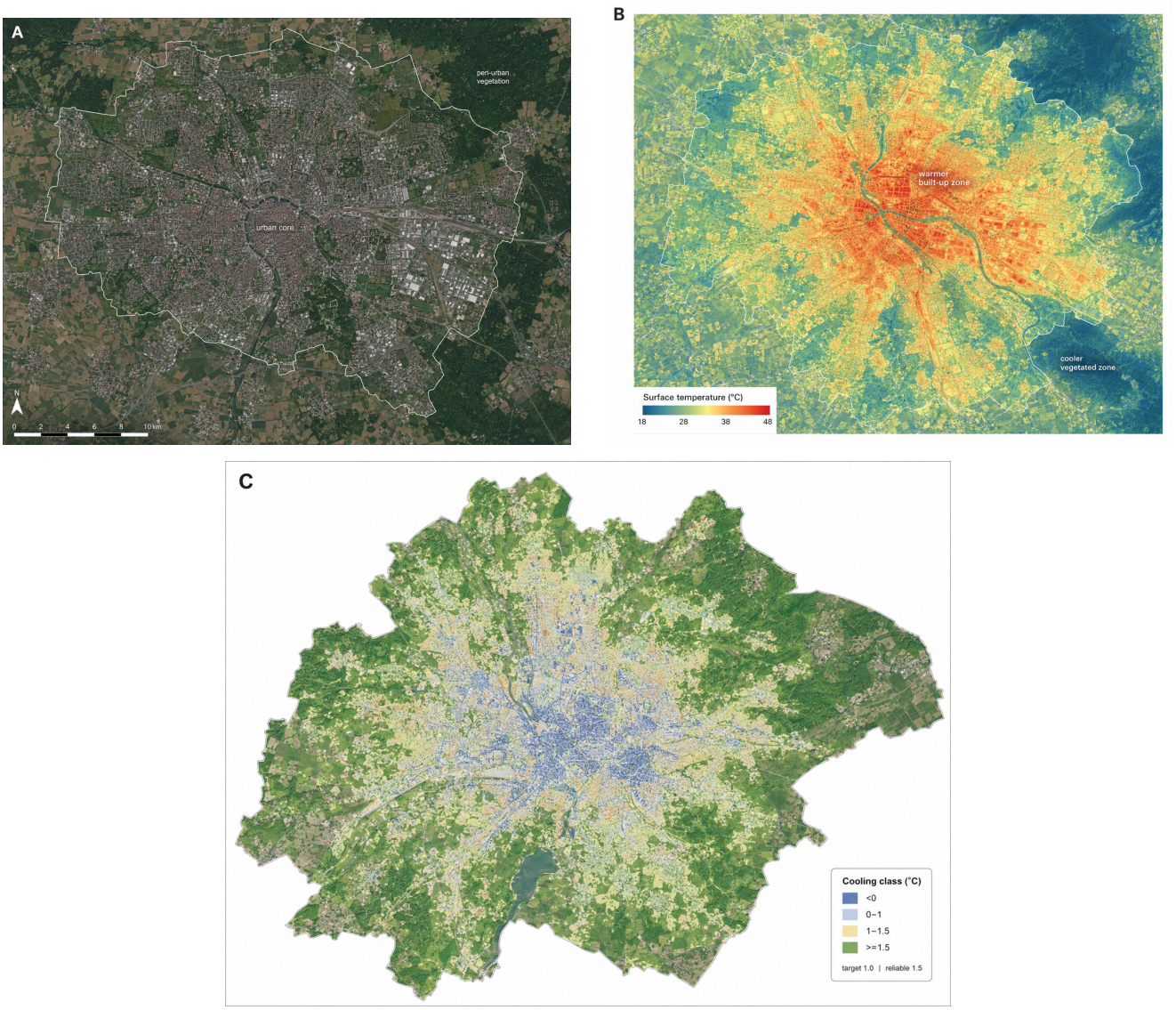

Figure 1. FUA surface context.

Three surface maps contribute to the article's target-oriented approach. Land cover is not sufficient for determining whether vegetation can meet cooling needs; surface temperature is not sufficient either because it does not show how much canopy is necessary to reach the goal. The planning object in the case study is a combination of urban land cover, vegetation, and thermal categories.

2. Materials and methods

2.1. European Functional Urban Area record

The numeric sample comprises 601 Functional Urban Areas of the EU-27, described in detail by Marando et al. [16]. Functional Urban Areas consist of an urban core with a population of 50,000 people and its commuting zone, thus making it appropriate to evaluate urbanized land in a whole rather than in the central part. This unit is especially helpful for studying urban heat adaptation since vegetative cooling may occur not only in dense cores but also in peri-urban zones. The other aspect of using Functional Urban Areas in heat analysis is the possibility of comparing results among different countries.

2.2. Thermal variables and validation

The source data for thermal calculations included median surface temperature of Landsat 8 OLI/TIRS images from July-August 2018, tree canopy density from the Copernicus High Resolution Layer for 2018, tree canopy water flux represented by transpiration and rainfall interception from the PML v2 evapotranspiration data set, and latitude. The population exposure to cooling effect was described by the global human settlement population density grid from 2015. After the harmonization process at 100 m spatial resolution, the water surfaces were removed since it was not necessary to analyze the cooling effect over water bodies. For validation of the air temperature model, 463 records from the NOAA station data base were used for the summer maximum air temperature. Adjusted R-square was 0.4, root mean squared error was 0.15 in degrees Celsius, scatter index amounted to 26 percent, and the prediction exhibited lower-value bias. Average error propagation was 0.5 °C.

The first stage of the calculation process is related to the two-level vegetation cooling model. First, land surface temperature is calculated as the function of tree canopy density and canopy water flux, and then maximum air temperature is estimated with the use of land surface temperature and latitude. The coefficients for the land surface temperature estimation model are the intercept at 35.89±4.89, slope for tree canopy density at -0.07±0.022, and slope for canopy water flux at -0.01±0.008. Coefficients for the air temperature estimation equation comprise the intercept at 40.63±0.44, slope for land surface temperature at 0.26±0.006, and slope for latitude at -0.52±0.008. Those values imply that the increase in tree canopy and canopy water flux decreases the land surface temperature term, while the air temperature transfer depends upon land surface temperature and latitude.

The process described visually in Figure 2 takes place in four stages corresponding to tree canopy, canopy water flux, land surface temperature, and cooling effect. Visual order reflects the real physical sequence of the process, where the effect of canopy cover and canopy water flux is exerted on surface temperature and then the surface thermal contrast is translated into air temperature.

Four panels provide the rationale behind treating canopy density and canopy water flux as complementary parameters for vegetation cooling evaluation. While canopy density has an impact upon incoming radiation and heat storage, canopy water flux indicates how much stored energy is converted into latent rather than sensible heat.

Table 1. European FUA inputs.

Component	Numerical content	Analytical role
Urban unit	601 Functional Urban Areas in the EU-27	Provides the comparable metropolitan unit for target attainment.
Thermal season	July–August 2018	Represents the summer period when UHI effects and vegetation cooling are most pronounced.
Spatial resolution	100 m land pixels	Preserves urban heterogeneity before aggregation to FUA values.
Cooling validation	463 NOAA stations; adjusted R^2 = 0.4; Scatter Index 26%	Provides the uncertainty context for reliable attainment.
Tree-cover rule	16%, 32%, 48% for 1, 2, 3 °C cooling	Converts target shortfall into canopy-equivalent shortage.
Population layer	Global Human Settlement population density for 2015	Links cooling benefit to residential exposure.

From Table 1, we can see that the assessment is neither based on one map nor on one mean value. Rather, it uses land temperature, canopy characteristics, canopy cooling, population, validation, and tree cover thresholds. All of these components are needed in order for the target to be properly interpreted – whether as surplus or shortfall – depending on uncertainties, canopy dosages, and population compatibility.

2.3. Target attainments and canopy shortfalls

In tree-canopy attainment analysis, the average cooling value for a Functional Urban Area serves as an initial condition. Denote C_i as the cooling effect of vegetation in an area i and τ as the cooling target. The target surplus can then be calculated using the formula:

$$S_i(\tau) = C_i - \tau. \quad (1)$$

If the surplus turns out to be positive, the FUA meets the specified target. Otherwise, the benefit provided by vegetation is below the cooling target, indicating a deficiency.

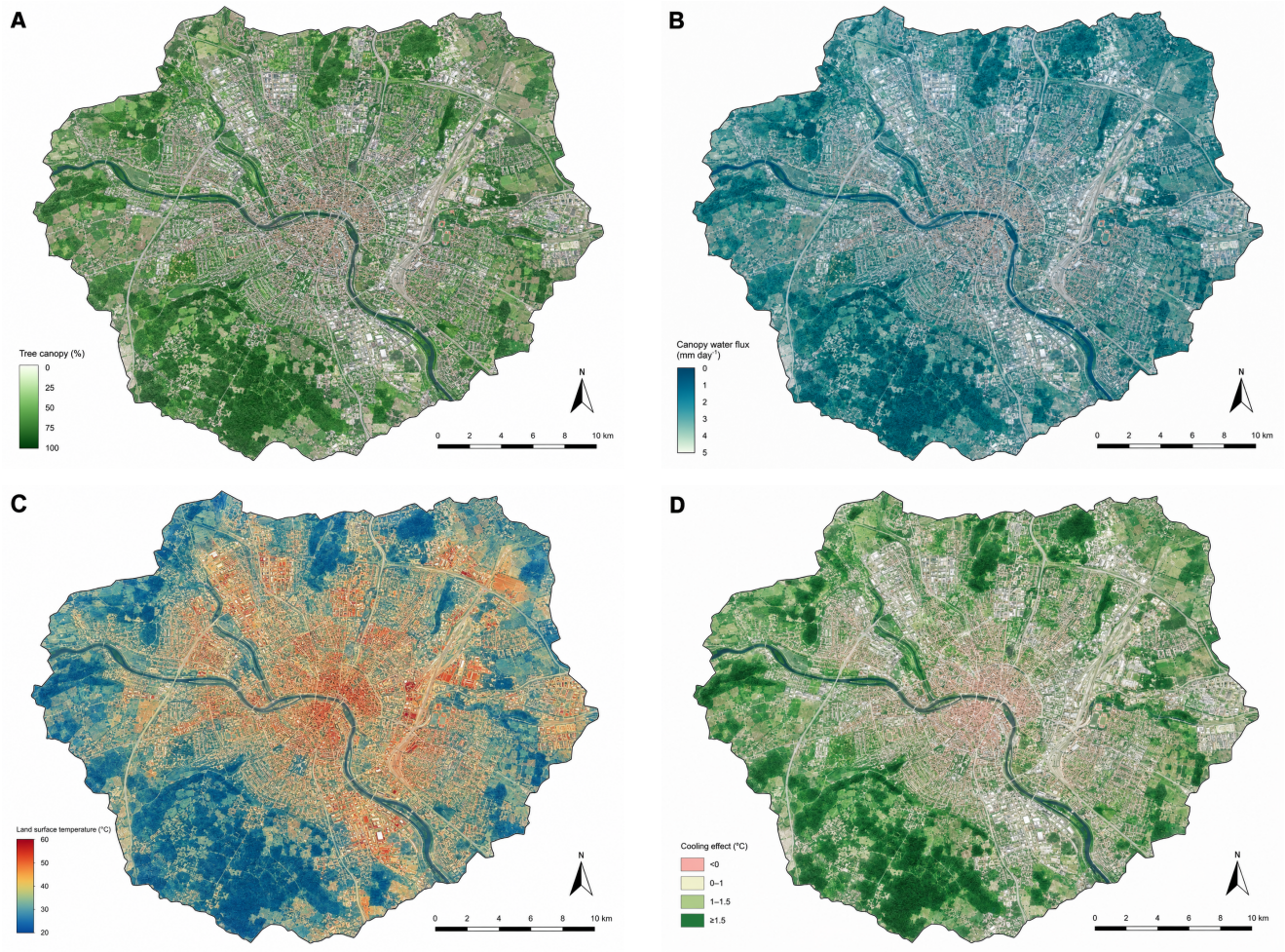

Figure 2. Cooling input surfaces.

Cooling shortfall can be determined by taking only the positive part of the expression:

$$D_i(\tau) = \max(0, \tau - C_i). \tag{2}$$

This equation yields zero whenever the FUA attains the target and provides a non-negative outcome otherwise. It makes sense to use such a formulation because adding up all of the below-target values does not allow one to subtract those of high-performing areas from them. For example, a city with strong cooling reserve cannot counterbalance the thermal problem of another city where vegetation cooling is weak.

The equivalent shortfall measured in tree cover percentage points will be:

$$G_i(\tau) = 16D_i(\tau). \tag{3}$$

This conversion follows the empirical rule where each percentage point of tree cover equals to one degree of average cooling. However, the resulting value should not be taken literally since it does not serve as the prescription for street and district plantings in any particular city. Rather, it can be seen as a screening parameter representing the cooling shortfall in a language understandable by land managers.

Attainments reliable within a certain threshold ϵ (equal to half of the propagated error) are:

$$R_i(\tau, \epsilon) = C_i - \tau - \epsilon. \tag{4}$$

With a one-degree target and a 0.5-degree threshold, the actual cooling should be at least 1.5 degrees to be considered reliable, one-degree attainment.

To calculate class averages, class percentages had to be converted into FUA counts by multiplying by 601 and rounding off to integer numbers. Shortage calculations required representative values of FUA cooling for each category: 0 °C for negative, 0.5 °C for 0–1 °C, 1.25 °C for 1–1.5 °C, 1.75 °C for 1.5–2 °C, and 2.45 °C for over 2 °C. For the high cooling class, this representative value is somewhat conservative since the FUA maximum is approximately 2.9 °C. Rounding off was needed only to convert continent-wide percentages into meaningful counts.

2.4. Error reduction and population agreement

A model's adequacy was assessed through two statistics: RMSE and Akaike Information Criterion for seven possible regression formulations. In order to determine the goodness of fit for various predictors and country-specific structure, the null hypothesis (model) had to be formulated. Model reduction relative to the null model can be expressed through the formula:

$$Q_j = 100\left(1 - \frac{RMSE_j}{RMSE_0}\right), \tag{5}$$

where Q_j represents a reduction in prediction error for model j in percent. Therefore, the value quantifies the model improvement compared to the no-predictors baseline.

To compare RMSE and AIC on a unified scale, the following measure can be used:

$$L_j = \frac{1}{2}\left(\frac{RMSE_j - RMSE_{\min}}{RMSE_{\max} - RMSE_{\min}}\right) + \frac{1}{2}\left(\frac{AIC_j - AIC_{\min}}{AIC_{\max} - AIC_{\min}}\right). \tag{6}$$

The lower is the loss, the better a model is in terms of predictive power and parsimony. This criterion serves exclusively for comparative purposes within this study since it prevents from selecting a model simply because it outperforms others in one aspect.

3. Results

3.1. Geographical distribution of summer cooling

According to the analysis of the dataset, vegetation cooling is abundant in Europe yet highly non-uniform. Overall, the mean value of cooling among 601 FUAs equals approximately 1.07 °C. In other words, it may seem that vegetation meets the one-degree target throughout the continent. However, such interpretation requires a more accurate approach. There are almost 9 Functional Urban Areas in the first category, approximately 272 in the second, around 208 in the third, roughly 91 in the fourth, and nearly 21 FUAs in the fifth class. This means that there are two substantial groups: one falling below the target and another being near it, not all satisfying it reliably.

These spatial characteristics are shown in the maps in Figure 3. Low-cooling cities are quite numerous in western and southern Europe, along with several coastlines, while intermediate and high cooling are typical for continental climates and those with larger green surrounding.

As can be seen from Figure 3, the most numerous class is the unreliable one rather than the class of attainments. Moreover, the largest number of FUAs belongs to the class with cooling ranging from 0 to 1 degrees, so the result is below the target. The following biggest one, with 1–1.5 °C of cooling, depends on the uncertainty. It means that European green infrastructure does provide cooling, yet some FUAs require further improvement.

The class conversion in Table 2 identifies 281 FUAs below 1 °C and 320 at or above that target. Once the reliability allowance is added, however, only 112 remain in the dependable group. The 208 FUAs between 1 and 1.5 °C are therefore the most policy-sensitive category: they are not failures, but they do not possess enough reserve to be treated as secure under uncertainty.

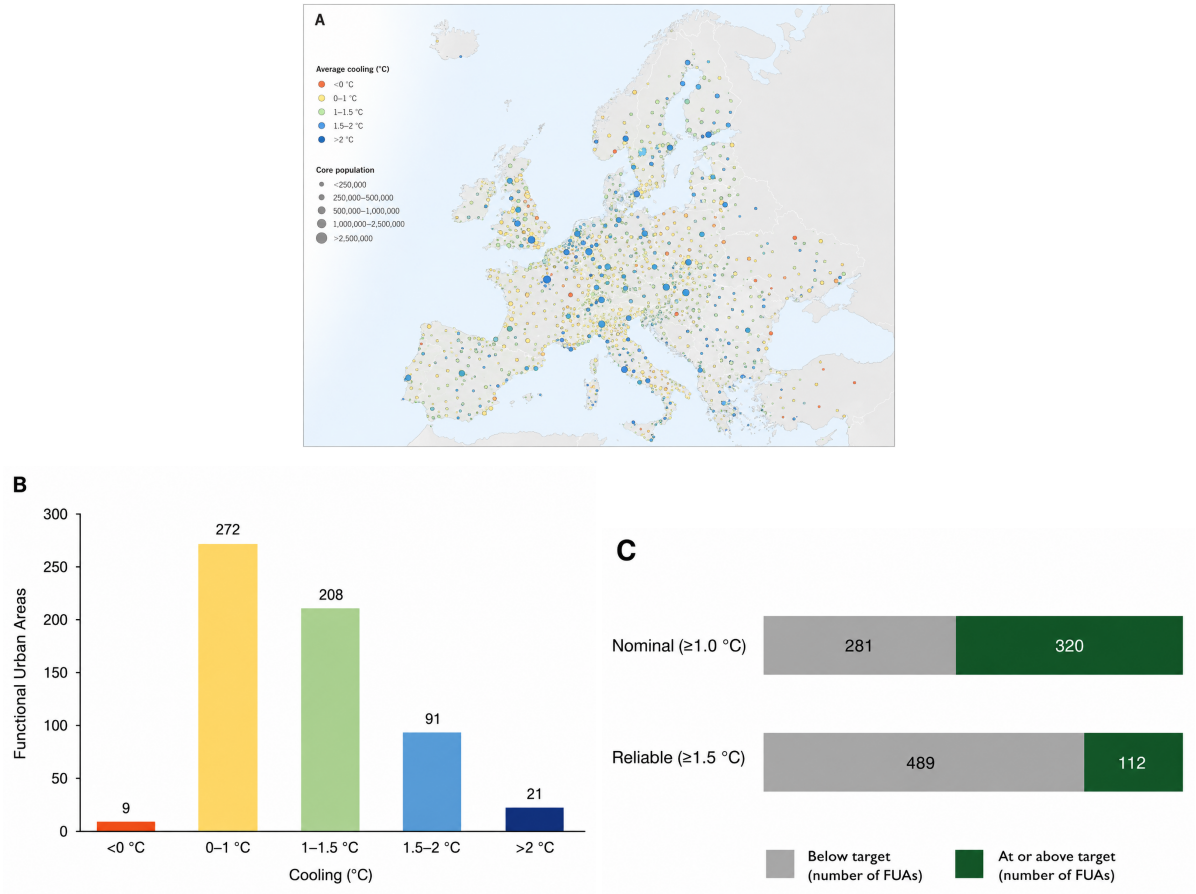

Figure 3. European cooling classes.

Table 2. Cooling attainment classes.

Cooling interval	Share of 601 FUAs	Approximate count	Target status at 1 °C	Planning interpretation
< 0 °C	1.5%	9	below target	adverse thermal sign
0–1 °C	45.3%	272	below target	insufficient vegetation cooling
1–1.5 °C	34.6%	208	nominal only	near-threshold reserve deficit
1.5–2 °C	15.1%	91	reliable	dependable one-degree attainment
> 2 °C	3.5%	21	high reserve	strong cooling surplus

3.2. Nominal and reliable cooling attainment

The shift from nominal to reliable status is isolated in Figure 4. The panels show how the same sample is read differently when the threshold moves from 1 °C to 1.5 °C. This is the most important numerical change in the article because it converts a majority nominal-attainment condition into a minority reliable-attainment condition. The change of vision in Figure 4 impacts the entire European data under the planning perspective. According to the nominal rule, 320 FUAs attain the one-degree line. According to the reliability rule, 208 FUAs attain the cautionary zone, whereas 112 continue to retain their reserves fully. This example indicates that the attainment needs to reflect on the inclusion of uncertainties.

3.3. Tree-cover requirements and shortage intensity

The shortage estimate in Table 3 helps understand how the one-degree target gets an interpretation within land management. The nominal shortage measured in canopy-equivalent FUA percentage points is equal to 2320. It is distributed predominantly in the 0–1 °C class because this temperature category consists of many FUAs; yet, this does not mean that all these FUAs are far away from the target. This outcome means that there is a priority in

expanding canopy area.

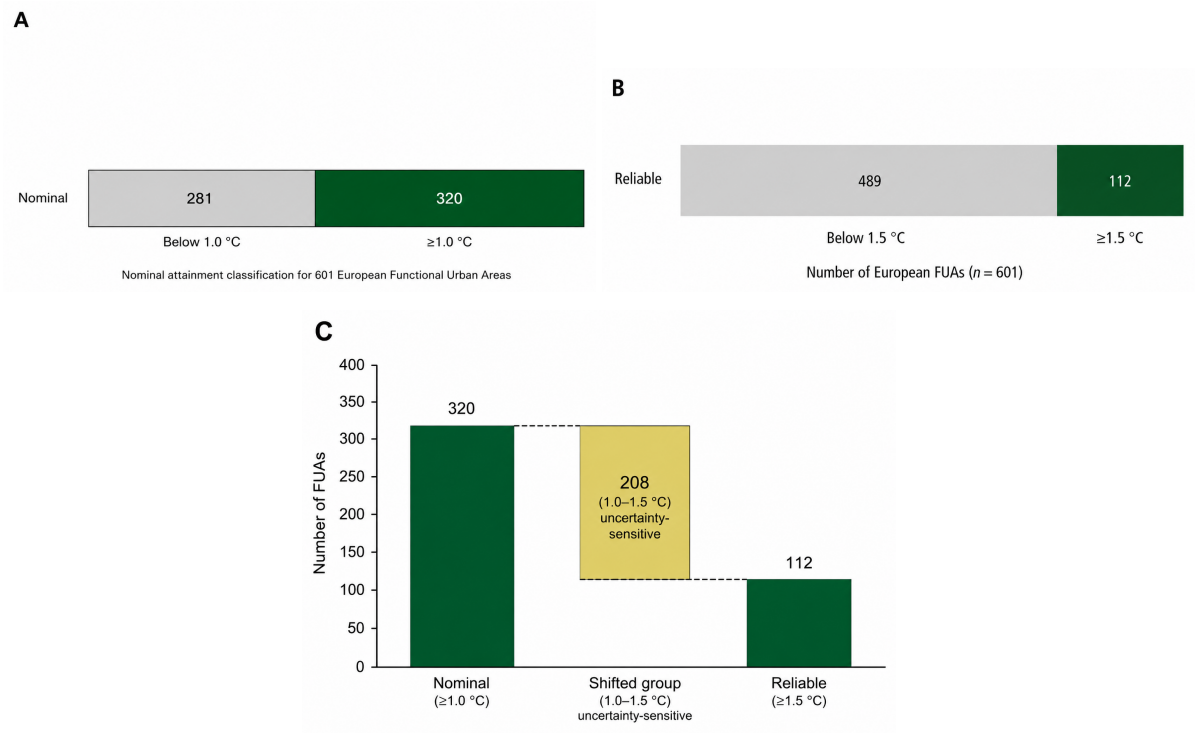

Figure 4. Attainment shift.

Threshold values shown in Figure 5 illustrate the target sequence graphically. The lower limit of sufficiency with 16% is a target value in case of achieving the goal to increase the temperature by 1 °C. On the other hand, the targets of two- and three-degrees correspond to 32% and 48% of tree cover, respectively. As a result, 32% of the total amount of European FUAs falls below 16%.

Table 3. Tree-cover-equivalent shortage.

Cooling class	Count	Representative cooling	Shortage to 1 °C	Canopy shortage per FUA	Class canopy shortage
< 0 °C	9	0.00	1.00	16.0	144
0–1 °C	272	0.50	0.50	8.0	2176
1–1.5 °C	208	1.25	0.00	0.0	0
1.5–2 °C	91	1.75	0.00	0.0	0
> 2 °C	21	2.45	0.00	0.0	0
Total	601				2320

The cooling sequence for tree cover from Figure 5 implies that the one degree of cooling is considered a minimal level of preparation while the two and three degrees of cooling require a share of the canopy which is not achievable by most dense urban areas using planting only. Such cities need to combine planting canopies with changes in surfaces, volume of soil, water retention, and conservation of mature trees.

From the comparison in Table 4, it is seen how fast shortage arises with an increase in the cooling target. While the one degree target splits a slight majority from a considerable shortage group, only 21 cities have managed to meet the two degrees target. The target for three degrees cooling is outside the observed range because the maximum value is 2.9 °C. Hence, increased cooling requires more than canopy planting.

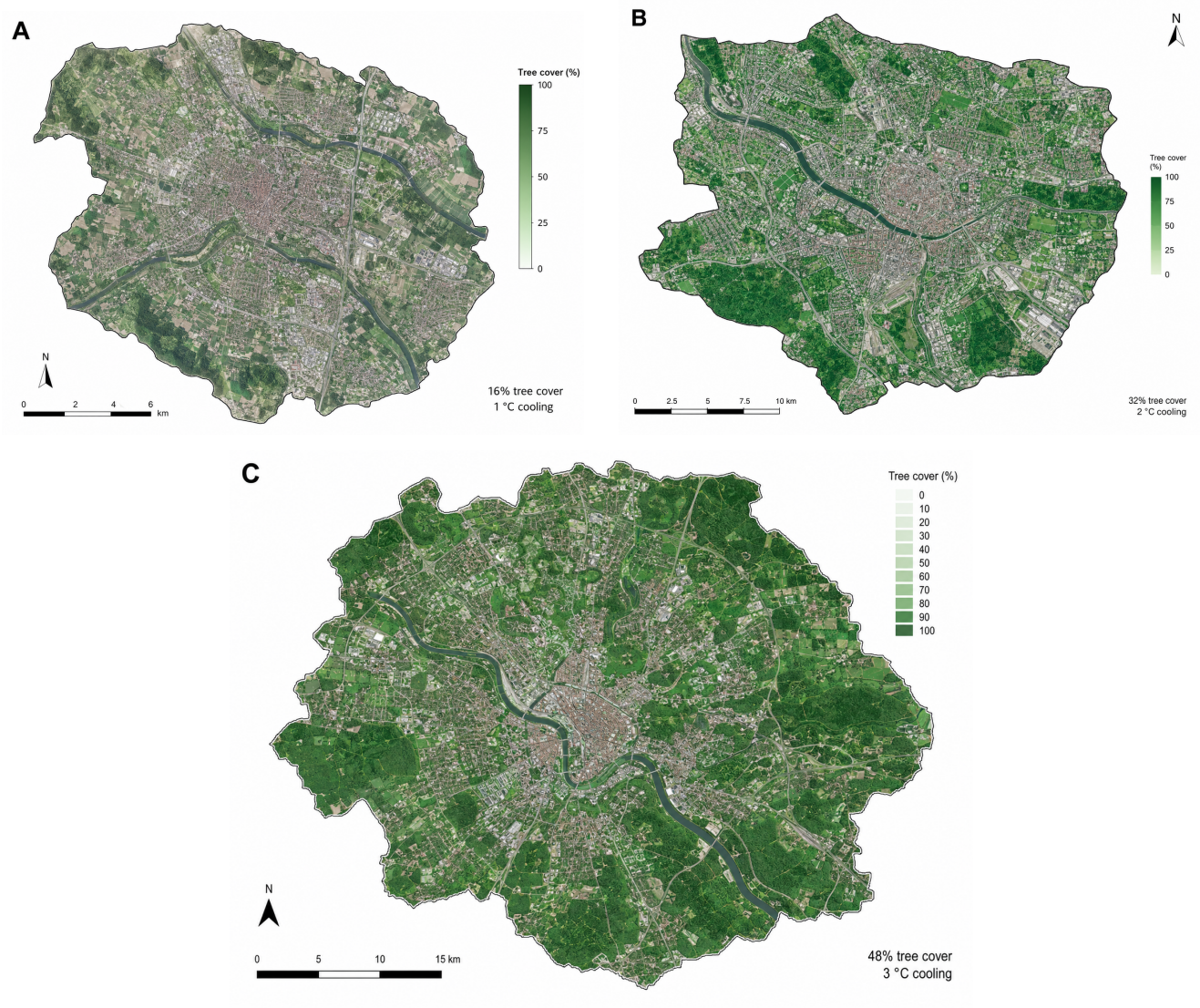

Figure 5. Tree-cover targets.

Table 4. Target intensity and estimated shortage.

Cooling target	Tree-cover reference	FUAs at or above target	FUAs below target	Approximate canopy-equivalent shortage
1 °C	16%	320	281	2320
1.5 °C reliable line	24% equivalent	112	489	5400
2 °C	32%	21	580	9676
3 °C	48%	0 within the observed FUA range	601	19141

3.4. Model adequacy and regional dependence

Model adequacy results support the use of country-conditioned interpretation. The null model has RMSE 0.9979 and AIC 1701.4. The best non-conditioned regression is weaker than country-conditioned alternatives. The fixed-effect model M4 gives RMSE 0.6999 and the lowest AIC, 1342.5, while the full mixed-effects model M6 gives the lowest RMSE, 0.6780, with AIC 1343.4. Relative to the null model, M6 reduces RMSE by about 32.1%, M4 by 29.9%, M5 by 25.6%, M1 by 22.9%, M2 by 17.5%, and M3 by 16.0%. These values show that national and regional structure carries important information for cooling prediction.

The panels in Figure 6 show that the most reliable interpretation does not come from a single universal regression. Country-conditioned models lie in the strongest region of the RMSE–AIC space, with M6 preferred for error and M4 preferred for parsimony. This supports a two-level planning stance: use a European target for communication,

but apply country-sensitive interpretation when estimating likely performance.

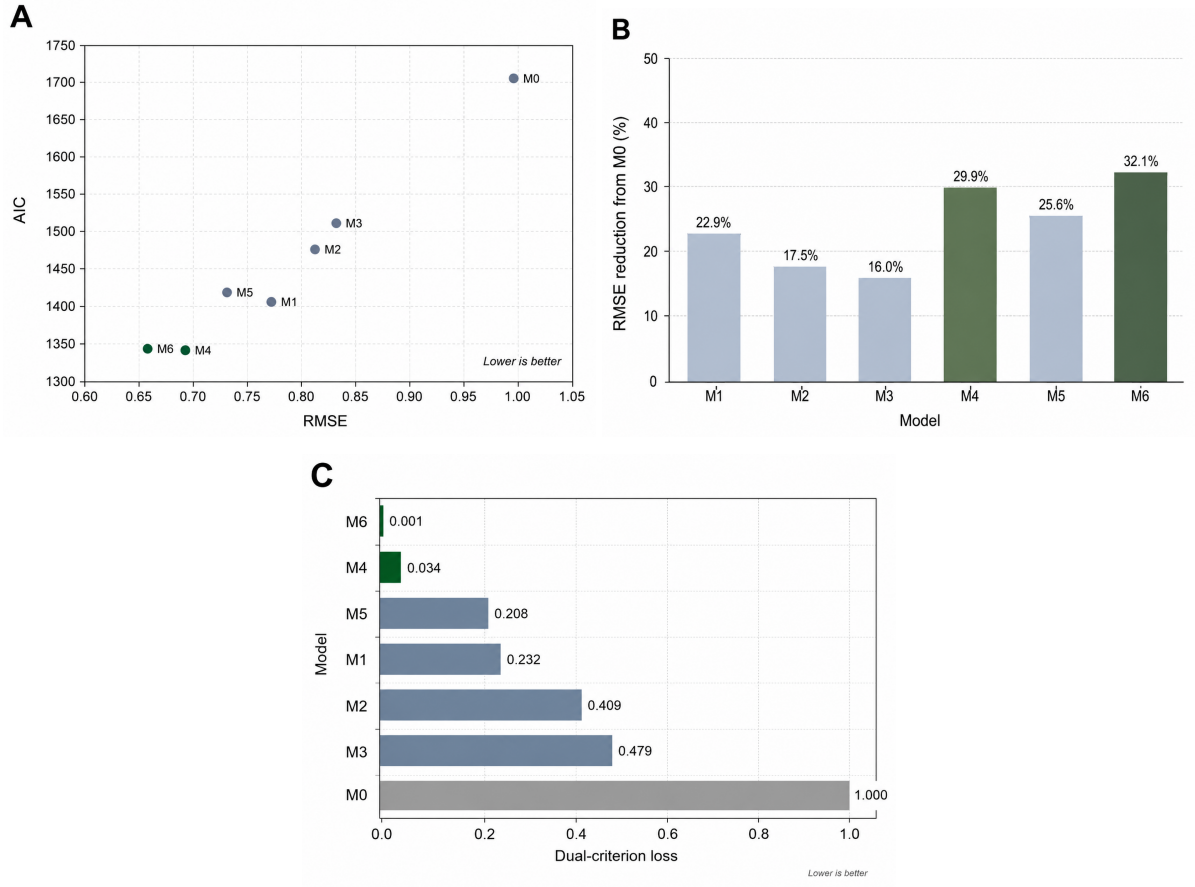

Figure 6. Model adequacy.

The results presented in Table 5 are significant for the interpretation of canopy targets. If tree-cover cooling were truly universal, then the tree-only model would predict values very close to those predicted by the country-conditioned models. It does not. Tree-cover is important, but its effects are conditioned by climatic, latitudinal, water, mixed cover, and urban-form factors in different countries. The tree-only target is still valuable as an introduction, while precise estimates must account for regionally specific conditions.

Table 5. Regression adequacy values.

Model	RMSE	AIC	RMSE reduction from M0	Selection distance
M0	0.9979	1701.4	0.0%	1.000
M1	0.7695	1406.1	22.9%	0.232
M2	0.8233	1473.0	17.5%	0.409
M3	0.8383	1506.5	16.0%	0.479
M4	0.6999	1342.5	29.9%	0.034
M5	0.7429	1419.3	25.6%	0.208
M6	0.6780	1343.4	32.1%	0.001

3.5. Beneficial population share and city comparisons

Beneficiary population share constitutes another criterion of the degree of attainment. In 63% of countries, more than half of the FUA population resides in territories with vegetation cooling being positive. For 37% of countries, the share of the population receiving a positive-cooling benefit is half or less. Hungarian and Cypriot populations

feature the highest median shares among FUA inhabitants benefiting from the effect, amounting to around 84% and 82%. Czechia and Bulgaria follow, with around 79% and 78% of people living in beneficial areas. Finns and Irish people feature considerably smaller median values, which amount to roughly 21% and 16%, respectively. A broad range can be seen for Spanish, Greek, Italian, Danish, and French citizens, with some territories having populations under 10% in beneficial cooling areas.

Population panels in Figure 7 separate exposure from attainment. Residents are classified as inhabiting beneficial areas regardless of FUA achieving a one-degree target. Such separation is vital for adaptation measures since beneficial cooling is only a necessary but not a sufficient criterion of heat relief during extreme weather conditions.

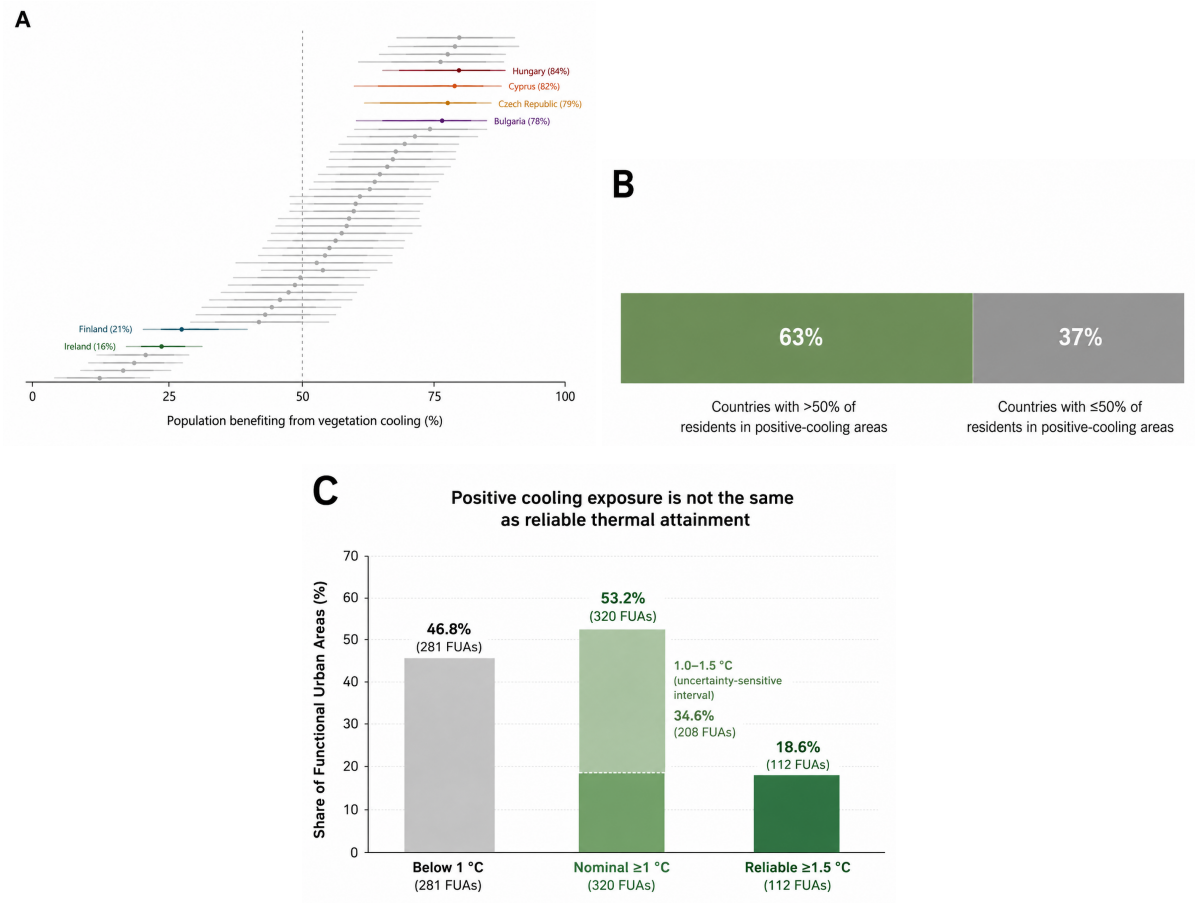

Figure 7. Population benefit.

Table 6. Country and capital signals.

Observation group	Specific values	Interpretation
High beneficiary countries	Hungary 84%, Cyprus 82%, Czech Republic 79%, Bulgaria 78%	Cooling and residential distribution are more strongly aligned.
Low beneficiary countries	Finland 21%, Ireland 16%	Positive-cooling land is less aligned with where residents live.
Countries with wide internal variation	Spain, Greece, Italy, Denmark, France	National averages should be treated cautiously.
Capitals with large negative-cooling share	Dublin 37%, London 31%, Copenhagen 31%, Athens 31%	Green space type, moisture, and urban morphology require closer diagnosis.
Capitals with large high-cooling share	Sofia 45%, Rome 43%, Riga 42% above 2 °C	Existing high-reserve canopy and peri-urban vegetation deserve protection.

The values in Table 6 show that population benefit and capital-city land composition do not follow a single European rule. Some capitals contain large shares of negative-cooling land, while others contain extensive high-cooling land above 2 °C. The same tree-cover target can therefore imply different actions: diagnostic repair where cooling is

negative, canopy distribution where residents are under-served, and mature-canopy conservation where high reserve already exists.

4. Discussion

4.1. Mean cooling and reliable attainment

The primary finding is that the European vegetation cooling effect cannot be described by the mean alone. With a mean FUA cooling of 1.07 °C, Europe just meets the target of 1 °C. Yet the class distribution shows that nearly half of the 601 FUAs are below this target value. Further, the number of FUAs within the 1–1.5 °C range and losing their secure status when a 0.5 °C allowance is considered stands at 208. The consequence is significant: While 320 FUAs meet the target of 1 °C in nominal terms, only 112 meet it reliably. This is the core numerical outcome of the Cooling Attainment Concordance approach. It transforms the promising mean value into a more careful assessment of attainment.

The class structure is consistent with the urban climate literature. Vegetation cooling relies on shading, evapotranspiration, surface change, and atmospheric exchange, and does not depend on mere vegetation pixels [29, 31**?**]. Tree canopy can reduce the radiant load and mitigate surface heating, while grass or low vegetation loses its effectiveness as soon as moisture conditions become limiting [26, 30]. The existence of a negative-cooling class in some southern coastal zones is thus physically plausible, and reflects the impact of drought, canopy structure, surface albedo, atmospheric stability, and shading of built cores [1, 5, 17, 37]. The practical implication is that negative or low vegetation cooling cannot be remedied by planting any vegetation on any available surface. It should be diagnosed and analyzed as a problem of canopy density, moisture availability, and surrounding surfaces.

4.2. Canopy thresholds and thermal performance

The tree-cover thresholds confirm this reading. The tree-share value corresponding to 1 °C cooling is 16%, and almost one third of all FUAs falls below the line representing this threshold. Such a tree-share value is not an ambitious ecological goal; it defines the minimum tree coverage needed for 1 °C cooling. The values required for 2 °C and 3 °C amounts are significantly higher, namely 32% and 48%. These are quite ambitious targets even for European cities because they imply a high level of canopy maturity, continuous canopy, inclusion of private property, school grounds, hospital gardens, and conversion of heat-retaining surfaces into vegetation cover.

The shortage numbers show why planners have to address the distribution of moderate deficits. The nominal shortage amount is about 2320 percentage-point-FUAs, and it stems entirely from the 0–1 °C class. Although these are not necessarily extreme cooling failures, they reflect extensive moderate deficiencies. Such a distribution pattern points to the necessity of systematic canopy improvement across many urban areas rather than individual showcase projects. Including the allowance in the calculation makes this issue even more salient since the near-threshold category is relatively large. Thus, FUAs in the 1–1.5 °C range should be viewed as sensitive areas subject to canopy loss, drought, or changes in land use that can shift them to the sub-target zone.

4.3. Regional calibration and population alignment

The conditional nature of country-dependent performance provides a clear planning application. The overall mixed-effects models, M6, yields the smallest root mean square error while the unconditional fixed-effect model, M4, has the lowest AIC. Thus, tree cover is indispensable in the explanation, but it alone is not enough to explain the effect. The difference in model performance represents country-specific effects of climate, urban form, vegetation condition, topography, maritime proximity, and history of heat adaptation. A general tree canopy target remains useful in communication, but a European-wide standard should be complemented by regional adaptation and calibration. While Mediterranean cities may need drought-resistant canopy and moisture retention facilities to sustain evapotranspiration, the northern cities may require different conditions, such as radiation, humidity, peatland surroundings, and seasonality of the temperature-vegetation relation [14, 20].

The population benefit provides a social dimension to the physical cooling distribution. Despite large cooling in some parts of a city, a country may find many citizens living in non-cooling regions. The median benefit levels illustrate the problem; thus, Hungary and Cyprus have values exceeding 80%, while Finland and Ireland remain far behind these countries, falling below 20%. The case with countries characterized by significant city-to-city variation is even more complicated since a national average may mislead planners. Thus, effective adaptation to urban heat should identify heat-exposed residential areas that are covered by vegetation cooling reserve.

Capital-city cooling signals show why classifications of this sort require local diagnosis. Dublin, London, Copenhagen, and Athens show large shares of negative-cooling areas despite the differences in climates, urban structures, and vegetation conditions. Each of them calls for individual analysis of green spaces, coastal conditions, and urban development. Dublin and Copenhagen may need more attention to the type of greenery, proximity to coast, and urban development pattern. London needs a closer examination of residential canopy inequality and heat-retentive urban surfaces. Athens requires moisture-preserving greening and resistance to canopy destruction due to Mediterranean drought. By contrast, Sofia, Rome, and Riga display large shares of cooling areas where cooling is greater than 2 °C. In these cases, apart from expanding canopy, it is necessary to preserve high-replacement canopy and green peri-urban areas.

4.4. Urban greening context and interpretation limits

Illustrations of urban form are shown in Figure 8. These maps put the numbers into an intuitive context and make the conclusion self-evident: Urban canopy needs to be evaluated according to the actual urban context rather than the canopy percentage alone.

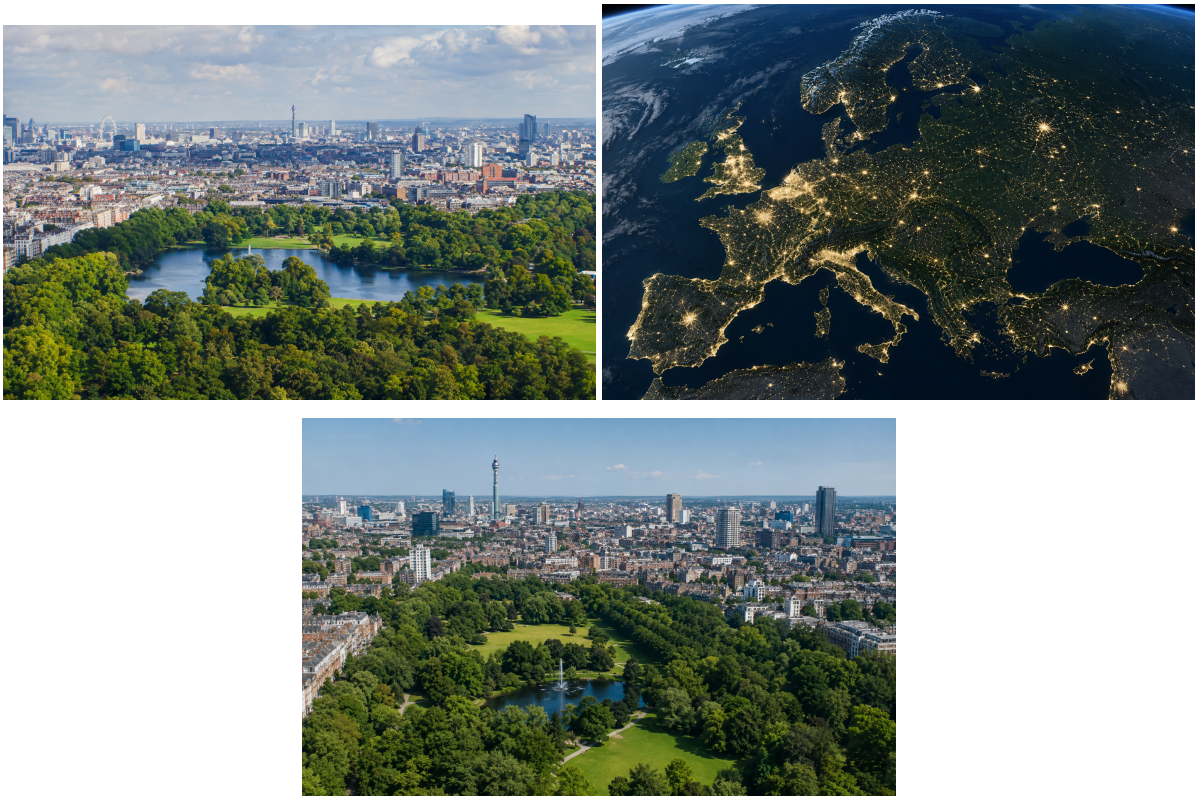

Figure 8. Urban greening context.

The examples in Figure 8 show how to interpret the quantitative results against an urban background. Extensive forest and parkland can be strong cooling reserves, but the residential districts may lack sufficient canopy coverage. For effective urban heat adaptation, both canopy protection and planting in heat-experienced residential areas are needed.

Several factors may influence interpretation and need to be acknowledged. The paper uses class-based data,

representative values, and coefficients, but not the full pixel-level grid. Percentage estimates are rounded, and interval representatives simplify the variation within classes. An uncertainty allowance of 0.5 °C relies on propagation of estimation error, yet actual values vary from city to city depending on conditions, land-cover composition, sensor operation, and model fitting. A 16% tree-cover share defines the minimum coverage rate, but in practice, urban vegetation may behave non-linearly if additional canopy is added to already covered districts or if canopy function is affected by moisture shortage. These factors do not detract from the method but define its scope and purpose as a continental-scale assessment instrument to be followed by local heat studies and urban greening planning.

In summary, the paper distinguishes four criteria that are often conflated in policy deliberation: positive cooling, target attainment, reserve, and population concordance. Positive cooling implies that vegetation delivers some cooling effect, while target attainment specifies the magnitude of this effect. Target attainment becomes reliable in the face of uncertainty, and concordance means that people actually experience cooling. Analyzing these issues separately contributes to clarity in heat adaptation planning and helps avoid exaggerated optimism about cooling averages.

5. Conclusions

The question of the paper was whether a cooling database for Functional Urban Areas in Europe can be turned into a planning diagnosis that distinguishes sufficient, marginal, and insufficient cooling of cities while considering tree cover demand, uncertainty, model accuracy, and population benefit. The answer is yes, but a reliable diagnosis proves to be more difficult than an average cooling value. European vegetation cools FUAs by 1.07 °C on average, yet approximately 281 out of 601 FUAs are still below a 1 °C cooling target. An additional 208 FUAs lie within the 1–1.5 °C range but do not represent a safe margin because of the 0.5 °C allowance for uncertainty. Only 112 FUAs meet the 1 °C cooling target reliably.

Tree cover analysis is equally straightforward. A 16% tree canopy is the minimum threshold associated with the 1 °C effect. The tree cover threshold for 2 and 3 °C corresponds to 32% and 48% of canopy cover. Approximately one third of FUAs fall short of the first threshold, while the nominal canopy equivalent shortage stands at about 2320 percentage-point-FUA units. If the 0.5 °C allowance is taken into account, then the shortage increases to 5400 percentage-point-FUA units due to the size of the near-threshold category. Model comparisons prove that a conditional model performs better than a fixed regression, implying that regional differences cannot be overlooked in canopy planning and that a European-wide target should be adapted regionally. A last caveat is raised regarding population benefit because cooling is unevenly aligned with residential distribution.

The conclusion is thus clear and specific. Tree canopy planning in Europe should not confine itself to the calculation of cooling averages or positive cooling only. The planning analysis should include four steps: classification of FUAs according to target attainment, cooling reserve, canopy equivalent shortage, and residential benefit. Areas that fall short of the 1 °C mark require canopy expansion and surface cooling. Those in the near-threshold region need canopy protection, drought resilience measures, and resistance to future densification. Above-threshold regions need canopy preservation and green peri-urban areas because they represent rare cooling reserves.

References

[1] Alonso, M. S., Fidalgo, M. R., & Labajo, J. L. (2007). The urban heat island in Salamanca (Spain) and its relationship to meteorological parameters. Climate Research, 34, 39-46.

[2] Koc, C. B., Osmond, P., & Peters, A. (2018). Evaluating the cooling effects of green infrastructure: A systematic review of methods, indicators and data sources. Solar Energy, 166, 486-508.

[3] Bates, D., Mächler, M., Bolker, B., & Walker, S. (2015). Fitting linear mixed-effects models using lme4. Journal of statistical software, 67, 1-48.

[4] Chrysoulakis, Nektarios, Sue Grimmond, Christian Feigenwinter, Fredrik Lindberg, Jean-Philippe Gastellu-Etchegorry, Mattia Marconcini, Zina Mitraka et al. "Urban energy exchanges monitoring from space." Scientific reports 8, no. 1 (2018): 11498.

[5] Clinton, N., & Gong, P. (2013). MODIS detected surface urban heat islands and sinks: Global locations and controls. Remote Sensing of Environment, 134, 294-304.

[6] European Commission. (2013). Green infrastructure (GI)—enhancing Europe's natural capital. Communication from the Commission to the European Parliament, the Council, the European Economic and Social Committee and the Committee of the Regions.

[7] Fischer, E. M., & Schär, C. (2010). Consistent geographical patterns of changes in high-impact European heatwaves. Nature geoscience, 3(6), 398-403.

[8] Founda, D., & Santamouris, M. (2017). Synergies between Urban Heat Island and Heat Waves in Athens (Greece), during an extremely hot summer (2012). Scientific reports, 7(1), 10973.

[9] Freire, S., MacManus, K., Pesaresi, M., Doxsey-Whitfield, E., & Mills, J. (2016). Development of new open and free multi-temporal global population grids at 250 m resolution. Population, 250, 33.

[10] Gong, P., Li, X., Wang, J., Bai, Y., Chen, B., Hu, T., ... & Zhou, Y. (2020). Annual maps of global artificial impervious area (GAIA) between 1985 and 2018. Remote Sensing of Environment, 236, 111510.

[11] Jansson, C. E. J. P., Jansson, P. E., & Gustafsson, D. (2007). Near surface climate in an urban vegetated park and its surroundings. Theoretical and Applied Climatology, 89(3), 185-193.

[12] Koppe, C., Kovats, S., Jendritzky, G., Menne, B., & Breuer, D. J. (2004). Heat waves: risks and responses. Copenhagen: Regional Office for Europe. World Health Organization.

[13] Maes, J., Zulian, G., Thijssen, M., Castell, C., Baró, F., Ferreira, A. M., ... & Teller, A. (2016). Mapping and assessment of ecosystems and their services. Urban ecosystems. In Mapping and assessment of ecosystems and their services. Urban ecosystems. (pp. 1-100). Publications office of the European Union.

[14] Manoli, G., Fatichi, S., Bou-Zeid, E., & Katul, G. G. (2020). Seasonal hysteresis of surface urban heat islands. Proceedings of the National Academy of Sciences, 117(13), 7082-7089.

[15] Marando, F., Salvatori, E., Sebastiani, A., Fusaro, L., & Manes, F. (2019). Regulating ecosystem services and green infrastructure: Assessment of urban heat island effect mitigation in the municipality of Rome, Italy. Ecological Modelling, 392, 92-102.

[16] Marando, F., Heris, M. P., Zulian, G., Udías, A., Mentaschi, L., Chrysoulakis, N., ... & Maes, J. (2022). Urban heat island mitigation by green infrastructure in European Functional Urban Areas. Sustainable cities and society, 77, 103564.

[17] Memon, R. A., Leung, D. Y., & Liu, C. H. (2009). An investigation of urban heat island intensity (UHII) as an indicator of urban heating. Atmospheric Research, 94(3), 491-500.

[18] Mentaschi, L., Duveiller, G., Zulian, G., Corbane, C., Pesaresi, M., Maes, J., ... & Feyen, L. (2022). Global long-term mapping of surface temperature shows intensified intra-city urban heat island extremes. Global Environmental Change, 72, 102441.

[19] Morabito, M., Crisci, A., Gioli, B., Gualtieri, G., Toscano, P., Di Stefano, V., ... & Gensini, G. F. (2015). Urban-hazard risk analysis: mapping of heat-related risks in the elderly in major Italian cities. PLoS one, 10(5), e0127277.

[20] Nouri, H., Borujeni, S. C., & Hoekstra, A. Y. (2019). The blue water footprint of urban green spaces: An example for Adelaide, Australia. Landscape and urban planning, 190, 103613.

[21] Oke, T. R. (1982). The energetic basis of the urban heat island. Quarterly journal of the royal meteorological society, 108(455), 1-24.

[22] Oke, T. R. (2002). Boundary layer climates. Routledge.

[23] Oke, T. R., Mills, G., Christen, A., & Voogt, J. A. (2017). Urban climates. Cambridge university press.

[24] O'Malley, C., Piroozfar, P., Farr, E. R., & Pomponi, F. (2015). Urban Heat Island (UHI) mitigating strategies: A case-based comparative analysis. Sustainable cities and society, 19, 222-235.

[25] Parastatidis, D., Mitraka, Z., Chrysoulakis, N., & Abrams, M. (2017). Online global land surface temperature estimation from Landsat. Remote sensing, 9(12), 1208.

[26] Potchter, O., Cohen, P., & Bitan, A. (2006). Climatic behavior of various urban parks during hot and humid summer in the Mediterranean city of Tel Aviv, Israel. International Journal of Climatology: A Journal of the Royal Meteorological Society, 26(12), 1695-1711.

[27] Qiu, G. Y., Zou, Z., Li, X., Li, H., Guo, Q., Yan, C., & Tan, S. (2017). Experimental studies on the effects of green space and evapotranspiration on urban heat island in a subtropical megacity in China. Habitat international, 68, 30-42.

[28] Core, T. (2023). R: A language and environment for statistical computing. R Foundation for Statistical Computing.

[29] Rahman, M. A., Armson, D., & Ennos, A. R. (2015). A comparison of the growth and cooling effectiveness of five commonly planted urban tree species. Urban Ecosystems, 18(2), 371-389.

[30] Saaroni, H., Pearlmutter, D., & Hatuka, T. (2015). Human-biometeorological conditions and thermal perception in a Mediterranean coastal park. International journal of biometeorology, 59(10), 1347-1362.

[31] Saaroni, H., Amorim, J. H., Hiemstra, J. A., & Pearlmutter, D. (2018). Urban Green Infrastructure as a tool for urban heat mitigation: Survey of research methodologies and findings across different climatic regions. Urban climate, 24, 94-110.

[32] Schiavina, M., Freire, S., & MacManus, K. (2019). GHS population grid multitemporal (1975, 1990, 2000, 2015) R2019A. European Commission, Joint Research Centre (JRC), 3.

[33] Schwarz, N., Schlink, U., Franck, U., & Großmann, K. (2012). Relationship of land surface and air temperatures and its implications for quantifying urban heat island indicators—An application for the city of Leipzig (Germany). Ecological indicators, 18, 693-704.

[34] Sebastiani, A., Marando, F., & Manes, F. (2021). Mismatch of regulating ecosystem services for sustainable urban planning: PM10 removal and urban heat island effect mitigation in the municipality of Rome (Italy). Urban Forestry & Urban Greening, 57, 126938.

[35] Shashua-Bar, L., & Hoffman, M. E. (2000). Vegetation as a climatic component in the design of an urban street: An empirical model for predicting the cooling effect of urban green areas with trees. Energy and buildings, 31(3), 221-235.

[36] Singh, P., Kikon, N., & Verma, P. (2017). Impact of land use change and urbanization on urban heat island in Lucknow city, Central India. A remote sensing based estimate. Sustainable cities and society, 32, 100-114.

[37] Sobrino, J. A., Oltra-Carrió, R., Sòria, G., Jiménez-Muñoz, J. C., Franch, B., Hidalgo, V., ... & Paganini, M. (2013). Evaluation of the surface urban heat island effect in the city of Madrid by thermal remote sensing. International journal of remote sensing, 34(9-10), 3177-3192.

[38] Taylor, J. R. (1980). An introduction to error analysis: the study of uncertainties in physical measurements. (No Title).

[39] Tiwari, A., Kumar, P., Kalaiarasan, G., & Ottosen, T. B. (2021). The impacts of existing and hypothetical green infrastructure scenarios on urban heat island formation. Environmental Pollution, 274, 115898.

[40] Tsiros, I. X. (2010). Assessment and energy implications of street air temperature cooling by shade tress in Athens (Greece) under extremely hot weather conditions. Renewable Energy, 35(8), 1866-1869.

[41] Venter, Z. S., Krog, N. H., & Barton, D. N. (2020). Linking green infrastructure to urban heat and human health risk mitigation in Oslo, Norway. Science of the total environment, 709, 136193.

[42] Wang, Y., & Akbari, H. (2016). The effects of street tree planting on Urban Heat Island mitigation in Montreal. Sustainable cities and society, 27, 122-128.

[43] Yoshida, A., Hisabayashi, T., Kashihara, K., Kinoshita, S., & Hashida, S. (2015). Evaluation of effect of tree canopy on thermal environment, thermal sensation, and mental state. Urban Climate, 14, 240-250.

[44] Zhang, X., Estoque, R. C., & Murayama, Y. (2017). An urban heat island study in Nanchang City, China based on land surface temperature and social-ecological variables. Sustainable cities and society, 32, 557-568.

[45] Zhang, Y., Kong, D., Gan, R., Chiew, F. H., McVicar, T. R., Zhang, Q., & Yang, Y. (2019). Coupled estimation of 500 m and 8-day resolution global evapotranspiration and gross primary production in 2002–2017. Remote sensing of environment, 222, 165-182.